

Van-der-Waals stabilized Rydberg aggregates

H. Zoubi,* A. Eisfeld, and S. Wüster

*Max Planck Institute for the Physics of Complex Systems,
Nöthnitzer Strasse 38, 01187 Dresden, Germany*

(Dated: 20 December, 2013)

Assemblies of Rydberg atoms subject to resonant dipole-dipole interactions form Frenkel excitons. We show that van-der-Waals shifts can significantly modify the exciton wave function, whenever atoms approach each other closely. As a result, attractive excitons and repulsive van-der-Waals interactions can be combined to form stable one-dimensional atom chains, akin to bound aggregates. Here the van-der-Waals shifts ensure a stronger homogeneous delocalisation of a single excitation over the whole chain, enabling it to bind up to six atoms. When brought into unstable configurations, such Rydberg aggregates allow the direct monitoring of their dissociation dynamics.

PACS numbers: 32.80.Ee, 37.10.Jk, 71.35.-y

Van der Waals (vdW) forces between ground state molecules or atoms can lead to the formation of molecular crystals and noble atom solids, without the need for electron sharing between the individual constituents. Optical and electrical properties in these aggregates are dominated by resonant interactions of transition dipoles which lead to the appearance of Frenkel excitons [1, 2], in which an electronic excitation can be delocalized in the lattice. Non-resonant interactions of vdW type lead to a change of the transition energies, since they affect the excited state differently than the ground state. This energy shift is homogeneous (i.e. the same for all monomers) for bulk crystals [3–5] and in this context is termed gas to crystal shift. For small structures of molecules, e.g. oligomers [6] or finite size domains on surfaces [7, 8], the shift is not homogeneous any more.

Here we show that this inhomogeneity of the vdW shifts can strongly influence the entire exciton wave function. To this end we consider assemblies of Rydberg atoms, which have huge transition dipoles (connecting two highly excited states) and hence can support Frenkel excitons over large distances [9, 10]. Under conditions of one-dimensional confinement we further demonstrate the possibility of self-assembled stable chains of Rydberg atoms, which form Rydberg-“aggregates” similar to the molecular situation [4]. The stable chain is formed by a competition between attractive forces generated by resonant dipole-dipole interactions and repulsive vdW interactions. This bears some similarities to eximers. For short chains (e.g. trimers) prepared in unstable configurations, we find an interesting break-up dynamics, reminiscent of molecular dissociation. Due to the exaggerated properties of Rydberg atoms, the dissociation can be directly monitored in real space.

The basic effect of the inhomogeneous vdW shifts can be understood by the following simple consideration. For comparatively large distances between Rydberg atoms in a chain, resonant dipole-dipole processes of the type: $ns + np \leftrightarrow np + ns$ are dominant [11, 12] and support

collective exciton states [9, 10, 13] which can have repulsive or attractive character [10]. If the distances between Rydberg atoms in a chain become shorter, off-resonant contributions to the system’s electronic energies increase and can be modeled by the addition of vdW potentials. This can give rise to on-site excitation energy shifts that depend on the geometry of the atomic assembly. For a trimer, for example, this effect can shift the central site out of resonance, since it has a different local environment than the outer sites. In attractive exciton states with repulsive vdW potentials, the site energy shifts near the chain center cause a stronger delocalisation of the excitation towards the chain edges. This results in much more homogeneous attraction throughout the chain, allowing the stabilization of attractive exciton states [10] by vdW repulsion. One-dimensional Rydberg chains can then essentially form bound states with many atoms, resembling the vdW bound self assembled molecular aggregates or molecular crystals. Previous work focused on just two Rydberg atoms, that can form bound molecular states in three dimensions [14–16].

For light Alkali atoms, atomic motion in the potentials discussed here can become relevant on the time-scale of Rydberg state lifetimes [17], resulting in flexible Rydberg aggregates [10, 18–20]. We investigate the behavior of such a flexible Rydberg trimer, and find that it may exhibit interesting dissociation dynamics that can be monitored in time and space due to the flexibility afforded by Rydberg physics.

We first analyze a frozen Rydberg aggregate, in which the positions $R_1, \dots, R_N \equiv \mathbf{R}$ of the atoms are assumed fixed and treat the electronic excited states of the system, where we use a simple model of N two-level Rydberg atoms. We define atomic states $|nl\rangle$, with principal quantum number n and angular momentum l , and concentrate on a lower Rydberg state $|s_i\rangle = |ns\rangle$ of energy E_s , and a higher Rydberg state $|p_i\rangle = |np\rangle$ of energy E_p . Here the index $i = 1, \dots, N$ labels the atoms. We consider the dynamics in the subspace spanned by the

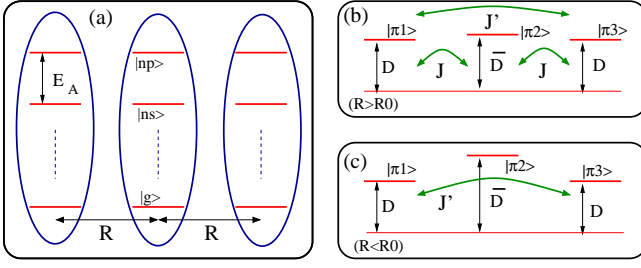


FIG. 1: (Color online) (a) Single body states of three Rydberg atoms are illustrated schematically. We show the $|ns\rangle$ and $|np\rangle$ states with the transition energy $E_A = E_p - E_s$, and the absolute ground state $|g\rangle$. (b) The states $|\pi_i\rangle$, with $(i = 1, 2, 3)$, are presented. For large interatomic distance relative to the crossover distance, $R > R_0$, the three $|\pi_i\rangle$ states are close to resonance, $D \approx \bar{D}$, and energy transfer is permitted among them with transfer parameters J and J' . (c) For small interatomic distance, $R_0 > R$, the states $|\pi_1\rangle$ and $|\pi_3\rangle$ have the same vdW shift of D , but $|\pi_2\rangle$ experiences a different shift \bar{D} with $\bar{D} \gg D$. Hence, the $|\pi_2\rangle$ state is no longer resonant with $|\pi_{1,3}\rangle$. Now energy transfer is allowed only among the $|\pi_1\rangle$ and $|\pi_3\rangle$ states with the transfer parameter J' .

states $|\pi_i\rangle = |s_1, \dots, s_{i-1}, p_i, s_{i+1}, \dots, s_N\rangle$, where only the i -th atom is in the (np) -state and all others are in the (ns) -state. In this subspace we write the relevant Hamiltonian as

$$H_{ex} = \sum_i E_i(\mathbf{R}) |\pi_i\rangle \langle \pi_i| + \sum_{ij} J_{ij}(\mathbf{R}) |\pi_i\rangle \langle \pi_j|, \quad (1)$$

where $J_{ij}(R_i, R_j) \propto 1/|R_i - R_j|^3$ is the resonant dipole-dipole interaction. It is responsible for transfer of excitation between states $|\pi_i\rangle$ and $|\pi_j\rangle$. The diagonal energies E_i contain the off-resonant vdW interactions. They can approximately be written as $E_i = E_0 + E_i^{(vdW)}(\mathbf{R})$, with $E_0 = E_p + (N-1)E_s$, and $E_i^{(vdW)}(\mathbf{R}) \approx h \sum_{\ell \neq i} C_6^{sp}/R_{i\ell}^6 + (h/2) \sum_{j \neq i} \sum_{\ell \neq i,j} C_6^{ss}/R_{j\ell}^6$, where $R_{i\ell} = |R_i - R_\ell|$, and h is the Planck constant. Here C_6^{ss} and C_6^{sp} denote the C_6 coefficients for the vdW interaction between two atoms in the s -state, and one atom in s and the other in p , respectively. With (1) we model only electronic quantum states and couplings that are relevant for the results presented here. They emerge in an essential state picture from a more complete diagonalisation of the atomic interaction Hamiltonian. For a discussion of three-body effects see [21].

Note that the magnitude and the sign of the C_6 coefficients depends on the chosen states (and atomic species). The resonant interaction J_{ij} depends in addition on the magnetic quantum number [9] which leads to an anisotropic spatial interaction. For the following considerations (where we restrict ourselves to one dimensional geometries) we ignore this anisotropy and write $J_{ij}(R_i, R_j) = hC_3/|R_{ij}|^3$, where C_3 can be both positive or negative.

Diagonalization of the Hamiltonian (1) for fixed po-

sitions \mathbf{R} leads to (adiabatic) eigenstates $|\psi_k(\mathbf{R})\rangle = \sum_{i=1}^N c_k^i(\mathbf{R}) |\pi_i\rangle$ and eigenenergies $U_k(\mathbf{R})$. To illustrate the basic electronic structure, we discuss the case of a finite linear chain of three Rydberg atoms with equal spacing R between nearest neighbors. The above excitonic Hamiltonian (1) can then be written in the basis $\{|\pi_1\rangle, |\pi_2\rangle, |\pi_3\rangle\}$, as

$$H_{ex} = E_0 + \begin{pmatrix} D & J & J' \\ J & \bar{D} & J \\ J' & J & D \end{pmatrix}, \quad (2)$$

where $J = \frac{hC_3}{R^3}$, and $J' = J/8$, with

$$D = \frac{h(C_6^{sp} + C_6^{ss})}{R^6} + D', \quad \bar{D} = \frac{2hC_6^{sp}}{R^6} + \bar{D}', \quad (3)$$

where $D' = hC_6^{sp}/(64R^6)$ and $\bar{D}' = hC_6^{ss}/(64R^6)$. Note that D' , \bar{D}' and J' are small and can often be neglected to a good approximation.

From Hamiltonian (2) it is apparent that the relevance of the relative shift $(\bar{D} - D)$ in the site energy of atom 2 is determined by the ratio of $J \sim R^{-3}$ and $(\bar{D} - D) \sim R^{-6}$, which depend differently on the distance between the atoms. In particular we consider two cases: large and small interatomic distances relative to the ‘crossover distance’, $R_0 \sim |(C_6^{sp} - C_6^{ss})/C_3|^{1/3}$, where the magnitude of J becomes of the order of $(\bar{D} - D)$. For $R > R_0$ the three states $|\pi_i\rangle$ with $(i = 1, 2, 3)$ are close to resonance and energy transfer is possible among them, as presented in Fig. 1 (b). Hence the three states can be coherently mixed to form excitonic states. In the case of $R < R_0$ the two states $|\pi_1\rangle$ and $|\pi_3\rangle$ are in resonance but the state $|\pi_2\rangle$ is shifted off resonance due to vdW interactions, as sketched in Fig. 1 (c). Now energy transfer is possible mainly among the states $|\pi_1\rangle$ and $|\pi_3\rangle$, which combine into excitonic states, while the state $|\pi_2\rangle$ remains a localized state. Thus, in this case the small J' cannot be neglected.

This can also clearly be seen in our numerical calculations. For these we choose parameters $C_3 = -1.16 \text{ GHz}(\mu m)^3$, $C_6^{ss} = 47 \text{ MHz}(\mu m)^6$, appropriate for a principal quantum number $n = 30$ [22], and $C_6^{sp} \approx +282 \text{ MHz}(\mu m)^6$. The latter might require external modification of interaction strengths with the use of Förster resonances [23, 24].

In Fig. 2 (a) we plot $U_k(R)$, for the three collective potentials (obtained by numerical diagonalisation of the Hamiltonian (2)) relative to E_0/h , as a function of the interatomic distance R . The lowest potential has a minimum around $R \approx 0.8 \mu m$, which leads to a bound state of the atoms. In Fig. 2 (b-c) we plot the fraction of each $|\pi_i\rangle$ state in the three collective states, with $(k = \alpha, \beta, \gamma)$, that is $|c_k^i|^2$, as a function of R . In mode α , for small distances the excitation is concentrated in the $|\pi_1\rangle$ and $|\pi_3\rangle$ states and the state $|\pi_2\rangle$ is almost not excited. For large

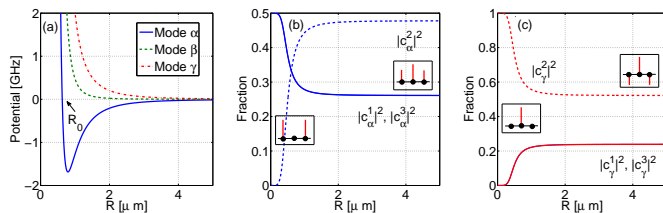


FIG. 2: (Color online) (a) The three collective potentials, U_k , as a function of the interatomic distance R . (b-c) The fractions $|c_k^i|^2$ as a function of the interatomic distance R . (b) In the first ($k = \alpha$), and (c) the third ($k = \gamma$) collective states. The insets include schematically the mixing amplitudes at the three $|\pi_i\rangle$ states for the first and the third collective modes at large distances, $R > R_0$, and small distances, $R < R_0$.

distances, a collective state is obtained with half the excitation fraction on the $|\pi_2\rangle$ state and a quarter on each of the $|\pi_1\rangle$ and $|\pi_3\rangle$ states. In mode β (not shown) the $|\pi_2\rangle$ state is never involved in the formation of the collective state. In mode γ for small R the excitation is almost entirely localized on the $|\pi_2\rangle$ state, the $|\pi_1\rangle$ and $|\pi_3\rangle$ states are not excited. For large R the γ state has the same population distribution as the α state. The amplitudes of the three $|\pi_i\rangle$ states are plotted schematically in the insets of Fig. 2 (b-c) for large and small R .

The situation is different when excitons are formed via dipole-dipole interactions involving ultracold ground- and low excited states in an optical lattice [25–27], or Rydberg states at larger separations than considered here [18, 19]. Then the vdW shifts discussed above are usually negligible.

After having established the effect of vdW interactions on the static properties of the exciton states in a chain of Rydberg atoms at fixed positions, we now consider dynamic properties of such a chain: a flexible Rydberg aggregate [20]. This is done by augmenting the total Hamiltonian of the problem with its kinetic energy part $\hat{H}_{\text{kin}} = \sum_i P_i^2 / (2M)$, where P_i is the momentum of the i 'th atom, and M its mass (for the examples shown, we choose Li). The combined treatment of exciton dynamics and atomic motion is involved quantum mechanically, but can be treated very well using Tully's quantum-classical description [10, 18, 19, 28]. In Tully's method, the internal electronic degrees of freedom are treated quantum mechanically, while the external position degrees of freedom of the atom are treated classically. The i 'th atom experiences a force $F_k^i = -\nabla_{R_i} U_k(\mathbf{R})$ according to one specific Born-Oppenheimer (BO) surface U_k . This surface corresponds to the k 'th eigenvector of the electronic Hamiltonian H_{ex} . Due to these forces we obtain time-dependent atomic trajectories $R_i(t)$ from the equation of motion $M \frac{d^2 R_i}{dt^2} = F_k^i$, and excitation amplitudes $c_k^i(t)$ from $i \partial_t |\Psi_k(t)\rangle = \hat{H}_{\text{ex}}(\mathbf{R}(t)) |\Psi_k(t)\rangle$, where $|\Psi_k(t)\rangle = \sum_i c_k^i(t) |\pi_i\rangle$. Stochastic non-adiabatic switches of the BO surface k are possible [28], but occur

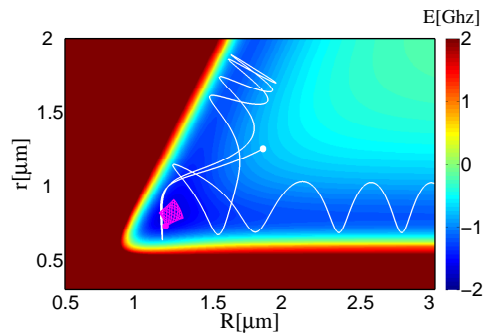


FIG. 3: (Color online) Energy landscape of Rydberg trimer aggregate [29]. Lines show a dissociating (white) and a stable (magenta) quantum classical trajectory. Big dots mark the starting position.

in a negligible fraction ($< 1\%$) of trajectories for all cases shown below.

We consider one-dimensionally confined Rydberg aggregates. First, we discuss a trimer aggregate (i.e. three atoms), where we focus on the potential surface which stems from the combination of a repulsive vdW interaction and an attractive ‘pure dipole-dipole surface’, as in the $k = \alpha$ state of Fig. 2 (a), since this may allow a stable configuration due to the potential minimum.

For a symmetric trimer the forces on the atoms can be solved analytically, in the general case the corresponding energy landscape has the shape shown in Fig. 3 [29]. It allows stable bound trimer-aggregates in the global minimum around $r \approx 0.8 \mu\text{m}$, $R \approx 1.2 \mu\text{m}$, as seen from the magenta trajectory.

The binding on the lowest Born-Oppenheimer surface can be extended to larger aggregates, as shown in Fig. 4 for the case of six atoms. Atomic initial position and momentum are randomly distributed, according to the quantum ground state of an initially harmonically confined particle. We then bin atomic positions $R_i(t)$ to obtain a total atomic density $n(x, t)$. It shows partial dissociation, but a signature of the six-atom aggregate clearly remains visible. This stabilisation crucially requires the modification of exciton states by the vdW shifts discussed earlier. Without them, the exciton wave function has insufficient amplitude on the outermost atoms and attraction of these atoms becomes too weak. We choose a Rydberg state $n = 30$ to maximize the product of self-trapping frequencies in the aggregate and system lifetime ($3 \mu\text{s}$ for the case shown). This empirically favors smaller principal quantum numbers.

Beside stable configuration one can prepare the system initially in configurations that exhibit a more complicated dynamics, e.g. the white trajectory shown in Fig. 3. Details for this trajectory are displayed in Fig. 5 (a-b). We can access regimes in which the trimer first undergoes breathing oscillations with excitation transfer be-

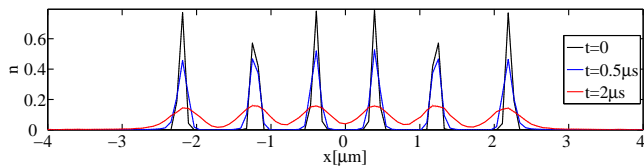


FIG. 4: (Color online) Total atom density n [arb.u.] in vdW stabilized Rydberg 6-mer for three selected times.

tween the sites, only to finally dissociate into a dimer and a free atom at a dissociation time $t_{\text{diss}} \approx 1 \mu\text{s}$, significantly faster than the excited system life-time of about $\tau_{\text{life}} = 6 \mu\text{s}$ [17].

The dissociation can also be studied in a trajectory average, where we obtain the pictures shown in Fig. 5 (c-e). Here, we consider a chain which is slightly perturbed from a symmetric configuration. The position of each atom is initially Gaussian distributed around $x = -1.5 \mu\text{m}$, $0.3 \mu\text{m}$, and $1.5 \mu\text{m}$. In the dynamics we can resolve some coherent motion of the chain in the total atomic density (Fig. 5 (c)), accompanied by excitation redistribution (Fig. 5 (d)). Later dissociation events that are qualitatively as in Fig. 5 (a,b) smear out the picture. Details of dissociation events depend strongly on the precise classical initial state, so that the multi-trajectory simulation shows a quite broad distribution of the final dimer energy [30]. The smallest dimer potential energy is $U_{\text{min}} \approx -1.2 \text{ GHz}$ and the largest initial total energy about $U_{0,\text{tot}} \approx -200 \text{ MHz}$, explaining the bounds of the energy spectrum in Fig. 5 (e).

One dimensional confinement of Rydberg atoms may soon be possible optically [31, 32], hence our system provides a platform for the direct visualization of wave-packet dynamics in an analog of molecular-dissociation processes, with the use of state-selective and high-resolution Rydberg atom monitoring schemes [33–36].

In conclusion, we addressed the formation of excitons in chains of Rydberg atoms with short separations, where vdW effect are shown to modify the resonant dipole-dipole picture. The level of excitation localization depends on the separation of atoms in the chain. We show that the combined action of vdW and resonant dipole-dipole forces can lead to interesting effects in one-dimensional chains, such as the stabilization of larger Rydberg aggregates in an attractive exciton. Even unstable parameter regimes show intriguing break-up dynamics, that can be followed experimentally in quite some detail in the realm of ultra-cold Rydberg physics. Moreover, using the HOMO and LUMO molecular configurations, similar exciton state modifications are expected for a cluster of organic molecules.

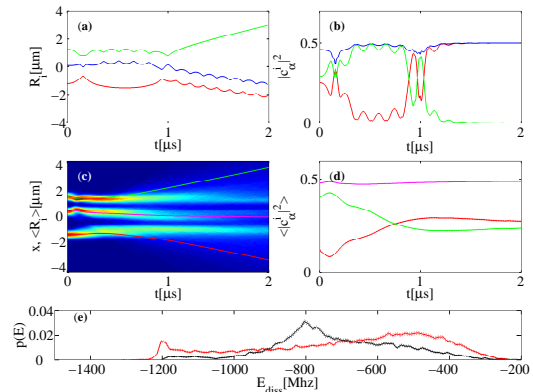


FIG. 5: (Color online) Rydberg aggregate dissociation for (a,b) symmetric and (c,d) asymmetric configurations. (a) Atomic positions R_i for single dissociating trajectory. (b) Excitation amplitudes $|c_\alpha^i(t)|^2$ for single dissociating trajectory. (c) Total atomic density n from trajectory average, overlaid are the mean position of the three atoms. (d) Mean excitation amplitudes $|c_\alpha^i(t)|^2$ on the three sites. (e) Energy distribution of the final-state dimer (black solid) and initial energy (red solid) for the same case as (c). The dotted lines indicate one standard error, and are nearly indistinguishable from the solid ones.

* Electronic address: zoubi@pks.mpg.de

- [1] J. Frenkel, *Zeitschrift für Physik A* **59**, 198 (1930).
- [2] J. Frenkel, *Phys. Rev.* **37**, 17 (1931).
- [3] S. Davydov, *Theory of Molecular Excitons* (Plenum, NY, 1971).
- [4] V. M. Agranovich, *Excitations in Organic Solids* (Oxford, UK, 2009).
- [5] H. Zoubi and G. C. La Rocca, *Phys. Rev. B* **71**, 235316 (2005).
- [6] J. Roden, A. Eisfeld, M. Dvořák, O. Bünermann, and F. Stienkemeier, *Journal of Chemical Physics* **134**, 054907 (2011).
- [7] M. Müller, A. Paulheim, C. Marquardt, and M. Sokolowski, *The Journal of Chemical Physics* **138**, 064703 (2013).
- [8] M. Müller, A. Paulheim, A. Eisfeld, and M. Sokolowski, *The Journal of Chemical Physics* **139**, 044302 (2013).
- [9] F. Robicheaux, J. V. Hernández, T. Topçu, and L. D. Noordam, *Physical Review A* **70**, 042703 (2004).
- [10] C. Ates, A. Eisfeld, and J. M. Rost, *New J. Phys.* **10**, 045030 (2008).
- [11] M. Saffman, T. G. Walker, and K. Molmer, *Rev. Mod. Phys.* **82**, 2313 (2010).
- [12] T. F. Gallagher and P. Pillet, *Ad. At. Mol. Opt. Phys.* **56**, 161 (2008).
- [13] S. Bettelli, D. Maxwell, T. Fernholz, C. S. Adams, I. Lesanovsky, and C. Ates, *Phys. Rev. A* **88**, 043436 (2013).
- [14] M. Kiffner, H. Park, W. Li, and T. F. Gallagher, *Phys. Rev. A* **86**, 031401(R) (2012).
- [15] M. Kiffner, W. Li, and D. Jaksch, *Phys. Rev. Lett.* **110**, 170402 (2013).

- [16] M. Kiffner, W. Li, and T. F. Gallagher, *J. Phys. B: At. Mol. Opt. Phys.* **46**, 134008 (2013).
- [17] I. I. Beterov, I. I. Ryabtsev, D. B. Tretyakov, and V. M. Entin, *Phys. Rev. A* **79**, 052504 (2009).
- [18] S. Wüster, C. Ates, A. Eisfeld, and J. M. Rost, *Phys. Rev. Lett.* **105**, 053004 (2010).
- [19] S. Möbius, S. Wüster, C. Ates, A. Eisfeld, and J. M. Rost, *J. Phys. B: At. Mol. Opt. Phys.* **44**, 184011 (2011).
- [20] K. Leonhardt, S. Wüster, and J. Rost (2013), (in preparation).
- [21] T. Pohl and P. R. Berman, *Phys. Rev. Lett.* **102**, 013004 (2009).
- [22] K. Singer, J. Stanojevic, M. Weidemüller, and R. Côté, *J. Phys. B: At. Mol. Opt. Phys.* **38**, S295 (2005).
- [23] E. Altieri, D. P. Fahey, M. W. Noel, R. J. Smith, and T. J. Carroll, *Phys. Rev. A* **84**, 053431 (2011).
- [24] J. Nipper, J. B. Balewski, A. T. Krupp, B. Butscher, R. Löw, and T. Pfau, *Phys. Rev. Lett.* **108**, 113001 (2012).
- [25] H. Zoubi and H. Ritsch, *Phys. Rev. A* **76**, 013817 (2007).
- [26] H. Zoubi and H. Ritsch, *Europhys. Lett.* **90**, 23001 (2010).
- [27] H. Zoubi and H. Ritsch, *Ad. At. Mol. Opt. Phys.* **62**, 171 (2013).
- [28] J. C. Tully, *J. Chem. Phys.* **93**, 1061 (1990).
- [29] For ease of interpretation we use Jacobi-coordinates $r = R_2 - R_1$, $R = R_3 - R_2 - r/2$.
- [30] We wait for the classical trajectory to have clearly dissociated, and then determine the kinetic plus potential energy of the dimer part of the system only.
- [31] L. Li, Y. O. Dudin, and A. Kuzmich, *Nature* **498**, 466 (2013).
- [32] R. Mukherjee, J. Millen, R. Nath, M. P. A. Jones, and T. Pohl, *J. Phys. B: At. Mol. Opt. Phys.* **33**, 184010 (2011).
- [33] A. Schwarzkopf, R. E. Sapiro, and G. Raithel, *Phys. Rev. Lett.* **107**, 103001 (2011).
- [34] B. Olmos, W. Li, S. Hofferberth, and I. Lesanovsky, *Phys. Rev. A* **84**, 041607(R) (2011).
- [35] G. Günter, M. Robert-de-Saint-Vincent, H. Schempp, C. S. Hofmann, S. Whitlock, and M. Weidemüller, *Phys. Rev. Lett.* **108**, 013002 (2012).
- [36] G. Günter, H. Schempp, M. R. de Saint-Vincent, V. Gavryusev, S. Helmrich, C. S. Hofmann, S. Whitlock, and M. Weidemüller, *Science* **342**, 954 (2013).